J. Physiol. (1985), **359**, 235–258
With 11 text-figures
Printed in Great Britain

PROFILES OF EVOKED RELEASE ALONG THE LENGTH OF FROG MOTOR NERVE TERMINALS

BY ALBERT J. D'ALONZO* AND ALAN D. GRINNELL

From the Department of Physiology, Ahmanson Laboratory of Neurobiology, and the Jerry Lewis Neuromuscular Research Center, UCLA School of Medicine, Los Angeles, CA 90024, U.S.A.

(*Received 26 July 1984*)

SUMMARY

1. In order to determine the relative probability of evoked transmitter release from different parts of frog motor nerve terminals, a technique has been developed in which single quantum end-plate potentials (e.p.p.s) are recorded by two intracellular electrodes, located at opposite ends of identified junctions. The log of the ratio of the amplitudes recorded simultaneously at the two electrodes is a linear function of the distance of the site of origin of the event from each of the two electrodes. Using on-line computer data acquisition and analysis, and current pulses at known locations for spatial calibration, it is possible to localize the site of single quantum e.p.p.s to within $\pm$ 10–20 μm.

2. Using the frog cutaneous pectoris neuromuscular preparation and a low calcium, high magnesium Ringer solution to ensure mostly single quantum events and failures, several thousand responses were recorded from each junction, allowing construction of a profile of the numbers of single quantum events arising from each portion of the junction. By comparison of junctional morphology and release profiles, it is possible to construct a probability of release per unit length profile for the entire junction. This technique has several advantages over localization of release events by measurements of extracellular synaptic currents.

3. It was found that, for most junctions, the central 60–90% of the terminal exhibited relatively uniform probability of release, with highest levels typically near the point where the axon first contacted the muscle fibre, or in regions with many short terminal branches. However, no instances have been found in which a small region of terminal (10% or less) showed extraordinarily high release levels (30–50% of the total release from the junction).

4. Characteristically, but not invariably, there is reduced release near the ends of terminal branches, especially the longer branches, where release per unit length could be as little as 5–10% of that in proximal portions.

5. Some junctions had large regions of terminal that released very little transmitter. These also showed multiple myelineated axonal inputs, and may have been polyneuronally innervated junctions in which one of the inputs was much weaker than the other.

* To whom correspondence should be sent.

6. No evidence was found for non-random clustering of responses or failures, or for coupled release of consecutive single quantum events from the same site at stimulus intervals of 40 ms or 1 s.

7. Absolute single quantum e.p.p. amplitudes were highly variable, but different branches or portions of branches of the same terminal showed similar means and variability, except near the ends of the junction, where there was sometimes a slight decrease in amplitude. There was no evidence for differing quantal size in different terminal branches, even in cases where the branches were releasing very different amounts of transmitter and may have come from different motoneurones.

INTRODUCTION

With the demonstration that there are 'active zones' located at regular intervals along the length of motor axon terminals (Couteaux & Pécot-Dechavassine, 1970; Heuser & Reese, 1973; Peper, Dreyer, Sandri, Akert & Moor, 1974), that fusion of vesicles appears to occur selectively at these sites during evoked transmitter release (Heuser, Reese, Dennis, Jan, Jan & Evans, 1979), and that quanta are released along the entire length of the terminal (Katz & Miledi, 1965; Wernig, 1976), it has been widely assumed that release is likely to occur with approximately equal probability from any active zone when an action potential invades the terminal.

Some findings, on the other hand, appear inconsistent with this view. Bennett & Lavidis (1979), for example, reported that an extracellular electrode at one location along the length of a toad motor nerve terminal could record as much as 30–50% of the total release from the terminal. This implies highly non-uniform release, although there was no correlation of physiology with terminal morphology in these measurements. In a subsequent paper, Bennett & Lavidis (1982) found less extreme non-uniformity, but still reported that in most terminals release was high within 60 μm of the end of the myelin sheath of the innervating axon, then fell off rapidly distal to this along each branch. Moreover, Vautrin & Mambrini (1980), working with frog sartorius and cutaneous pectoris junctions, found that single quantum evoked responses were clustered at discrete latencies, suggesting that release was occurring only at certain spots along the terminal. Thus, there are interesting claims of non-uniformity in release.

We feel that it is important to resolve these issues for two reasons. First, an understanding of the mechanism(s) of transmitter release is critically dependent on correlates of ultrastructure and release. Secondly, it is becoming increasingly clear that transmitter release is a plastic phenomenon. Not only do terminals continue to grow as muscle fibres increase in size (Kuno, Turkanis & Weakly, 1971; Bennett & Pettigrew, 1975; Harris & Ribchester, 1979; Nudell & Grinnell, 1982, 1983), but even in adult animals there is a continuing process of terminal growth and retraction (remodelling), apparently as a function of hormonal state or activity level (Wernig, Pécot-Dechavassine & Stover, 1980). It is appropriate to ask whether transmitter release changes accordingly. Moreover, simple experimental manipulations such as reduction in the size of the target (Herrera & Grinnell, 1980; Pockett & Slack, 1982) or axotomy of contralateral homologous motoneurones (Herrera & Grinnell, 1981) can cause sharp increases in transmitter release from motor nerve terminals, without evident change in the length or light microscopic appearance of the terminals. Even

within the same muscle, different terminals may differ by more than 20-fold in release per unit length, without apparent differences in structure at the light microscopic level (Grinnell & Herrera, 1980, 1981). Thus, both normally and as a result of plastic changes, there is reason to believe that different terminals or portions of terminals may appear similar but show differential probabilities of release.

We felt it was important to determine whether release probability is relatively uniform throughout the length of a terminal, or can, in fact, be highly non-uniform, with 'hot spots' of release that are more numerous or more 'active' in stronger terminals. To do this, we have adapted and developed a technique used by Gundersen, Katz & Miledi (1981) to study the effects of botulinum toxin on release. This involves recording intracellularly at both ends of a terminal to determine the ratios of the single quantum end-plate potential (e.p.p.) amplitudes seen at the two sites. Because e.p.p. amplitude falls predictably with distance, different ratios correspond to different points of origin between the two electrodes. This technique has allowed us to identify the site of release to within $\pm$ 10–20 μm, and permits us to conclude that, at least in most terminals, release per unit terminal length differs by no more than 2–4-fold over much of the length of a terminal, with no evidence that one or a few sites are responsible for most of the release. On the other hand, there is a marked tendency for decreased release from the distal ends of terminal branches. In some cases, large portions of terminals, probably representing weak inputs from second axons, show much lower levels of release. A preliminary report of this work has appeared (D'Alonzo & Grinnell, 1982).

METHODS

The cutaneous pectoris (c.p.) nerve–muscle preparation from *Rana pipiens* (body length 5–7 cm) was selected for these experiments. Muscles were pinned at 110% of their resting length in Sylgard-lined Petri dishes and superfused in a low calcium Ringer solution containing (mM): NaCl, 116; KCl, 2; $NaHCO_3$, 1; $CaCl_2$, 0·3–0·4; $MgCl_2$, 5–6 and HEPES, 5 (pH 7·2) to ensure a majority of e.p.p.s of unit quantal size. In addition, neostigmine methylsulphate (20 μM) was added to this solution to increase the size of responses. Recordings were made at 15 °C.

The present study takes advantage of the cable properties of muscle fibres, and the potential for extremely accurate discrimination of amplitude differences using on-line computer data acquisition and analysis. A single quantum e.p.p. decreases in amplitude exponentially from the site of origin as predicted by the cable properties of the fibre and the temporal properties of the e.p.p. current (Hodgkin & Rushton, 1946; Jack, Noble & Tsien, 1975). The ratio of the amplitudes recorded intracellularly on either side of the junction permits determination of the relative distance of the site of origin of the response from each of the two electrodes. When the response arises near one end of a terminal, the electrode near that end records a large response, the distant electrode a smaller response. An e.p.p. arising halfway between the two electrodes would be recorded with equal amplitude at both, assuming uniform cable properties along that length of the fibre. The shorter the length constant of the fibre and the larger the signal-to-noise level, the more accurate the technique. In practice, the length constant and the degree of accuracy achieved must be determined empirically in each fibre, using calibration techniques described below.

On-line recording methods

Responses were evoked by stimulation of the whole c.p. nerve via a suction electrode at a frequency of 1–1·25 Hz, which was found not to lead to obvious changes in quantal content during the course of an experiment. Fibres were chosen with junctions on the upper surface, so that the ends of the junction could be visualized at 400 × with Hoffman amplitude modulation optics. When the preparation had equilibrated for 30 min in low calcium, high magnesium Ringer solution, a single electrode was inserted intracellularly into the muscle fibre just beyond one end of the nerve terminal. If most events were single quantum e.p.p.s or failures, and the resting potential was

acceptable (−85 mV or higher), a second recording micro-electrode was inserted just beyond the other end of the terminal (Fig. 1). Each electrode was filled with 0·6 M-K_2SO_4, 1 mM-KCl, and 50 mM-EDTA, this being found to result in stable recordings with quiet noise level, minimal tip potential and an acceptable electrode resistance (approximately 40 MΩ). Data acquisition and analysis was via an on-line Lomas microcomputer (see below). Each electrode fed into its own physiological amplifier (Biodyne Electronics AM-2), with the output sent through two circuits: one

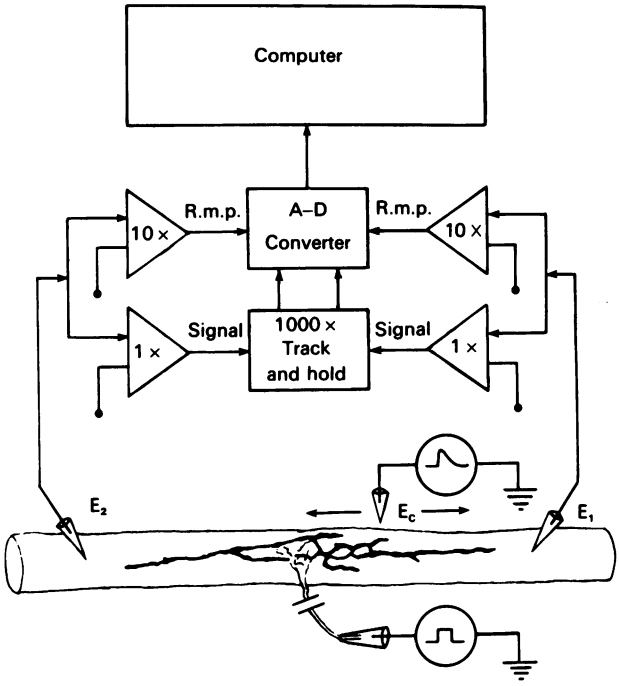

Fig. 1. Schematic representation of the experimental design. Evoked responses and muscle fibre resting membrane potential (r.m.p.) were recorded by intracellular electrodes E_1 and E_2 and fed via an analog-to-digital converter into a computer where data were stored and analysed. Ratios of the unit quantal response amplitudes (E_1/E_2) were used to determine the site of release along the length of the end-plate. After 3000–5000 stimuli, a current-passing electrode (E_c) was inserted into the muscle fibre at known locations. Electrotonic pulses generated by E_c and recorded at E_1 and E_2 were similar in size and shape to unit quantal responses. Ratios of the amplitudes of these artificially generated events were used to calibrate ratios with sites of origin. For a detailed description see text.

used to measure the resting potential at the time of each response, the other sent to the computer through a track and hold circuit that allowed for the subtraction of the resting potential from each of the responses. Signals were amplified 1000 × by this circuit to bring them into the voltage range appropriate for computer analysis. All four inputs (resting membrane potential and responses at each electrode) were digitized via a 12-bit analog-to-digital converter (TECMAR S-100 AD212), sampling each input every 100 μs.

Each record was analysed in the following manner. The base line prior to the stimulus artifact was sampled every 100 μs for 5 ms, and averaged. Beginning 100 μs after the stimulus artifact, the signal was sampled for 20 ms, a peak value found, and the best parabolic fit made for all the points within a 2–3 ms window centred around the peak. Then an accurate measure of the peak amplitude was calculated from these points by subtracting the base line from the peak value as determined by the curve of best fit. The following parameters were obtained: stimulus number, peak amplitude

of the e.p.p. recorded at electrodes E_1 and E_2, standard deviation of each base line, standard deviation of the parabolic fit of the peak, and resting membrane potential recorded by each electrode. In order to obtain an adequate number of single quantum e.p.p.s, 3000–5000 records were obtained from each fibre. Once these values had been obtained, the relationship between response position and relative amplitude at the two electrodes was calibrated. This was achieved by penetrating the fibre with a third micro-electrode at two or three different known distances between the two electrodes (using a calibrated eye-piece reticle and local landmarks), and at each point passing 200–300 current pulses of amplitude and form similar to the single quantum end-plate current, producing voltage responses similar to those arising through evoked release.

Histology

It is necessary in each case to know accurately the morphology of the nerve terminal studied, at least at the light microscopic level. Hence, at the end of each experiment muscles were rinsed with normal frog Ringer solution, fixed (2 % glutaraldehyde in normal frog Ringer solution for 30 s) and then stained for nerve terminals with the Nitroblue tetrazolium method of Letinsky & DeCino (1980) and for post-synaptic acetylcholinesterase (AChE) by the method of Karnovsky (1964). A careful camera lucida drawing was made of the terminal at 400 × *in situ* with a water immersion objective, and where there was any ambiguity about terminal structure the fibre was dissected from the muscle and the junction drawn again at 400 × with an oil immersion objective. Our measurements of terminal morphology were based upon only the enlarged branches associated with post-synaptic AChE deposits, not the much finer processes not associated with AChE, that sometimes connect different branches. Sites of recording electrode penetration, also stained dark blue by the Nitroblue tetrazolium treatment, were noted. The camera lucida drawing of the terminal was then divided into 10 μm bins on linear graph paper for further correlation with physiology.

Data analysis

After the experiment the digitized records were reconverted to millivolts and amplitudes were corrected for drifts in resting potential. Experiments were used only if an adequate number of records were obtained in which membrane potentials did not fall below −75 mV (or 70 mV in cases of large responses and a good noise level). Experiments were also rejected if the membrane potential recorded by the two electrodes differed by more than 4 mV. For data that met these criteria, the ratios of the e.p.p. amplitudes recorded by the two electrodes were calculated. In practice, these ratios (E_1/E_2) ranged from approximately 0·6 to 1·7.

Calibration records were similarly analysed and, knowing the position of the current passing electrode in each case, an accurate correlation between amplitude ratios (E_1/E_2) and inter-electrode distance could be determined. This was done by plotting ln (E_1/E_2) *versus* number of events, as in Fig. 2. An inter-electrode distance could then be assigned to any given ratio by plotting a linear regression of ln (E_1/E_2) *versus* distance. These calibrations normally yielded highly accurate linear relationships ($r > 0{\cdot}95$) (see calibration curves of Figs. 4–9). The length constant of a frog muscle fibre to a constant current pulse is approximately 2 mm (Katz, 1948). However, for transient voltage changes, the length constant is much shorter (in our experiments approximately 900 μm) (Jack *et al.* 1975). Since a change in location of origin simultaneously reduces the recorded amplitude at one electrode, and increases it at the other, plotting the ratios of the amplitudes recorded at both electrodes effectively halves this length constant to a figure of around 450 μm, which was approximately the electrode separation used in these experiments. This degree of change in ratio with distance is sufficiently steep to make our technique feasible.

Once a calibration curve was constructed and the expected ln (E_1/E_2) for each 10 μm bin was known, we then determined which evoked potentials were unit quantal and had a satisfactory signal-to-noise ratio. The first step in this selection was to plot a histogram of the sum of the E_1 and E_2 amplitudes for all records (Fig. 3). From this plot we could eliminate failures and multiquantal events, as well as calculate the quantal content by the method of failures (del Castillo & Katz, 1954). To eliminate virtually all the multiquantal events, all summed e.p.p.s greater than approximately 1·3 times the mode of the unit quantal peak were excluded. (Multiquantal events must be excluded, since simultaneous release of quanta from different sites would yield uninterpretable E_1/E_2 amplitude ratios.) In addition, data that might have been artifactual, due for example to overlap of an evoked event with a miniature e.p.p. (m.e.p.p.) or to unusual noise at

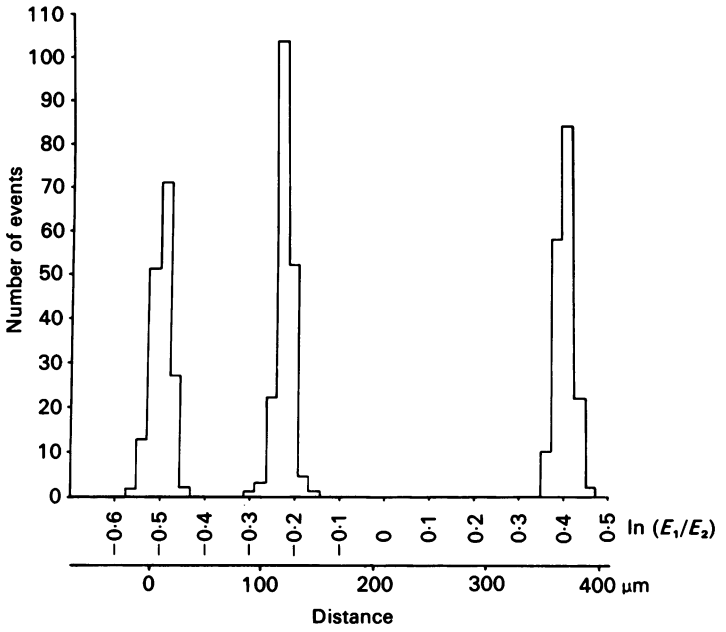

Fig. 2. Calibration ratios derived from three different E_c locations in a sample experiment. The histogram shows the number of events correlated with the logarithm of the ratio of the response amplitudes (ln (E_1/E_2)) recorded at E_1 and E_2. The X-axis contains scales for distance in μm and ln (E_1/E_2) values, showing how ratios correlate with distance. From these calibration points an estimate of the accuracy of the technique can also be made (see text for a more complete description).

the time of the response, were eliminated by rejecting any records in which the standard deviation of the values for the base line, or of the parabolic fit to the response peak, exceeded approximately 0·05 mV. What remains is a population of unit quantal sized e.p.p.s. An examination of the ratios (ln (E_1/E_2)) obtained from single quantum-evoked responses supports our conclusions regarding the accuracy of this technique. Usually fewer than 2 % of the observed ratios lay outside the range of ratios corresponding to the terminal borders as predicted by the calibration curve.

To determine the amount of release from each portion of the junction, the calibration curve was used to determine the ln (E_1/E_2) amplitude ratios which corresponded to the ends of the junction, and a histogram was made which divided this range of ratios into the same number of equal sized bins as there were 10 μm bins of end-plate length. Thus, each bin of ratios corresponded to a 10 μm bin of fibre length. This is not the same as 10 μm of terminal length, of course, since there were often several branches present within that 10 μm portion of muscle fibre. For accurate comparison of release with morphology, therefore, the summed length of all terminal branches within cholinesterase-outlined gutters within each 10 μm length of fibre was measured and plotted. These plots then could be converted into the percentage of total release and of total length per 10 μm bin (see panels *C* and *D* of Figs. 4–9). The absolute number of events localized to each bin was then divided by the amount of terminal within that bin, and the ratio expressed as a percentage of the summed release per unit length of all bins, which we define as the probability of release per unit length. Different terminal branches or portions of branches sometimes differ significantly in width, and release might be expected to vary accordingly (Kuno *et al.* 1971). However, over most of the range of apparent terminal widths, as measured by light microscopy, there is no clear-cut correlation between width and release levels (Nudell & Grinnell, 1982; A. A. Herrera, A. D. Grinnell & B. Wolowske, unpublished). There *is* a correlation between area of pre- and post-synaptic apposition, measured ultrastructurally, taking into account the degree of terminal invagination into the fibre and the amount of Schwann cell interposition (Herrera, Grinnell & Wolowske, 1983;

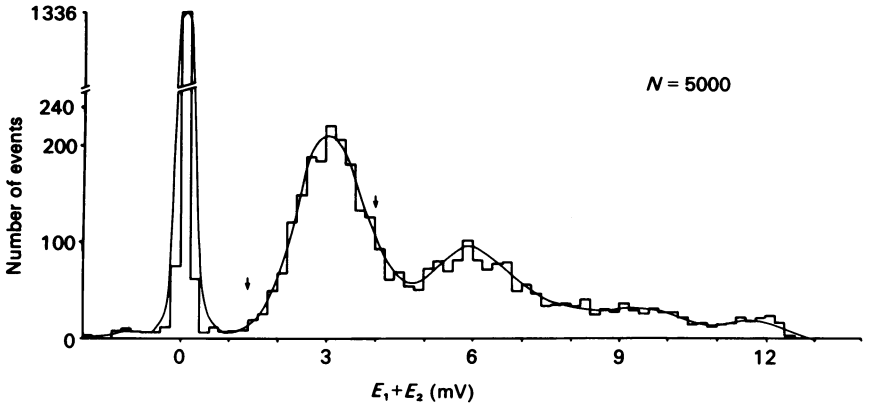

Fig. 3. Sample distribution of summed response amplitudes ($E_1 + E_2$) used to identify failures and single or multiquantal events. Since the selection of single quantum events preceded determination of site of origin of events, comparing summed amplitudes from both electrodes provided a convenient means for estimating the relative amplitudes of different responses. The centring of failures at approximately +200 μV reflects computer measurement of the peak of the noise level in the system. Selection of single quantum e.p.p.s was done by eye, by eliminating 'events' below the base of the first response peak, and greater than 1·3 times the mode of the first peak, since many responses greater than this value were likely to be multiquantal (see arrows). The numbers of single, double and triple events were accurately predicted from the number of failures and followed a Poisson distribution (del Castillo & Katz, 1954). The smooth curve was fitted to the histogram by eye.

A. A. Herrera, A. D. Grinnell & B. Wolowske, unpublished data). However, it was not feasible to determine these variables in our experiments. Therefore, we avoided using terminals in which there were obvious disparities in apparent terminal width, and otherwise used terminal length as the criterion of terminal size.

Accuracy of the technique

Although we have subdivided our data into 10 μm bins, we are fully aware that the accuracy of the technique is not as precise as that. As can be seen in Fig. 4, even for calibration pulses generated at a single location a range of ln (E_1/E_2) value was recorded spanning 4–6 bins. However, normally 40–50% of the ratios fell within 1 bin, with a further 20–25% in each of the directly adjacent bins. No more than 5–10% of the ratios fell as much as 2 bins distant from the mean. Knowing the expected ln (E_1/E_2) for any given inter-electrode distance, it was thus possible to predict the ratios that would be observed for release from any given portion of the nerve terminal. In most cases, using the methods described, we were able to localize the site of any given unit quantal event with an accuracy of approximately $\pm$ 10–20 μm. For each junction, we have plotted the observed percentage release per unit length within each 10 μm bin (heavy-lined histograms, panel *E*, Figs. 4–9; see also Fig. 10). In addition, however, to better reflect the actual accuracy of localization of release, we have recalculated this value after making the approximation that 50% of the events recorded in a given bin actually arose within that bin, and 25% came from the 10 μm bin to either side (see dashed lines, panel *E*, Figs. 4–10). For the end bins, it is assumed that there was zero probability of release from the next adjacent bin beyond the end of the terminal. The effect of this approximation is to analyse all data within a 'weighted' moving 30 μm bin, with each 10 μm bin value representing the most accurate value obtainable for the centre 10 μm portion of a 30 μm region.

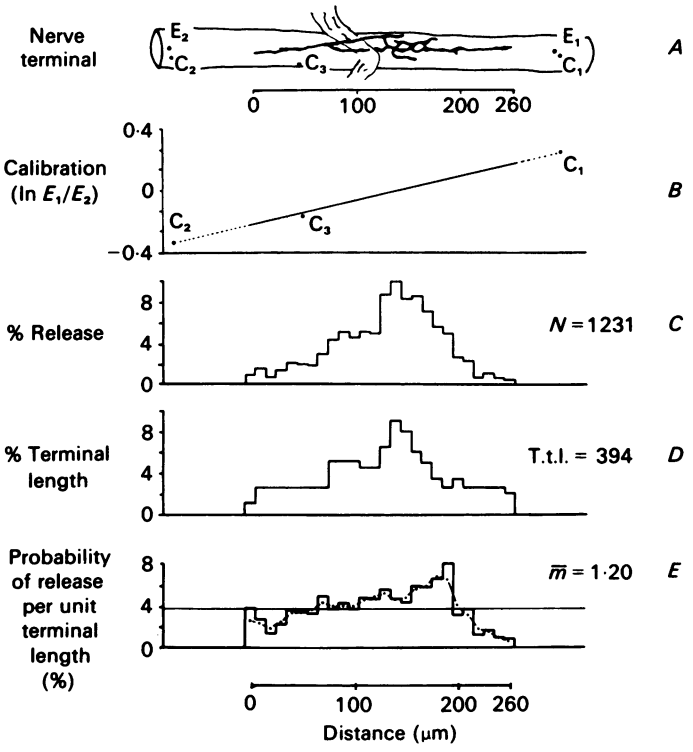

Fig. 4. Correlation of morphology and release properties in a 'simple' junction. *A*, a camera lucida drawing of a muscle fibre with its nerve terminal. Also shown are the positions of recording electrodes E_1 and E_2 and the position and order of calibration pulses (C_1, C_2 and C_3). This drawing is used to construct a histogram of the percentage terminal length per 10 μm of fibre length (*D*). A histogram of the percentage release (*C*) is aligned with the terminal length by means of a calibration curve (*B*). The histogram of *E* is obtained by dividing the absolute number of events per 10 μm bin by the total amount of terminal within that bin, expressed as a percentage of the summed release per unit terminal length for all bins. The dashed line represents a weighted moving-bin correction to this histogram, based on the assumption that 50% of the events are localized to any one bin and 25% come from each adjacent bin (see text). The horizontal line represents the expected probability of release per unit terminal length had release been perfectly uniform from all portions of the terminal. Values for total number of events (*N*), total terminal length (t.t.l.) and mean quantal content ($\bar{m}$) are given. It is noteworthy that *C* and *D* mimic one another and that release near the point of nerve entry tends to be higher than release distally.

RESULTS

Release profiles

Figs. 4–10 present the data derived from nine different representative junctions, using the methods outlined above. The junction shown in Fig. 4 was the one from which the specific examples in the Methods section were taken. In considering our results, it is convenient to group junctions into three categories, based on their structure: simple, complex and possibly polyneuronally innervated.

Simple junctions. The fibres presented in Figs. 4 and 5 each had relatively simple

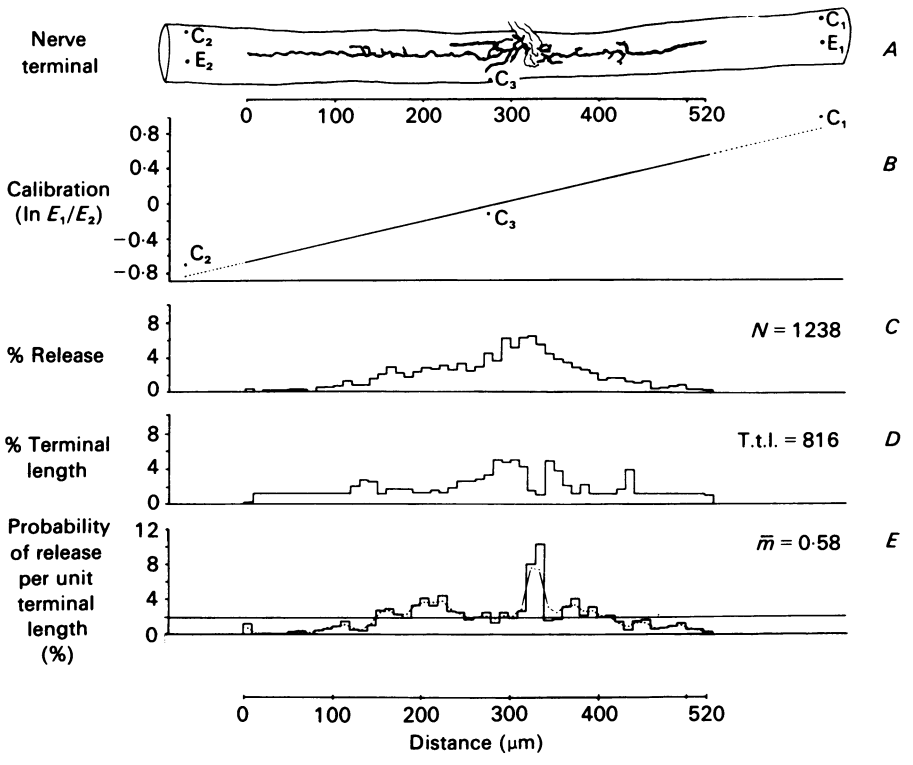

Fig. 5. A 'simple' junction displaying long lengths of terminal with minimal amounts of branching. As in Fig. 4 there is good correlation between *C* and *D*, except at 320–340 μm. However, the high level of probability of release per unit terminal length (*E*) at 320–340 μm is largely artifactual, due to spilling of events from adjacent bins into a 20 μm region having very little terminal (see text for a detailed explanation). Release per unit length is relatively uniform throughout the central region of the end-plate, but is gradually reduced at the distal ends. (For a more complete explanation refer to the legend of Fig. 4.)

terminal geometry, allowing us to analyse the probability of release unambiguously over considerable lengths of single nerve terminal branches. As is evident from inspection of panels *C* and *D* in these two Figures, the profiles of release and terminal length were quite similar, each showing a preponderance of both terminal and release near the mid-region of the terminal, where the myelinated axon ended. The similarity of the morphology and release profiles immediately suggests that the release probability per unit length, at low calcium concentrations, is relatively uniform. This result was characteristic of all simple junctions studied ($n = 6$). However, it is obvious that release was not entirely uniform. In the junction shown in Fig. 4, for example, release per unit length fell off sharply in the distal 20 % of its length at the right (E_1) end, to about 40 % of the amount expected if release had been completely uniform. This decrease was counterbalanced by an elevated release probability in the central region of the junction. In the junction shown in Fig. 4 there was only a slight drop at the left (E_2) end. On the other hand, the example shown in Fig. 5 is more characteristic in showing a pronounced drop in release probability at both ends of

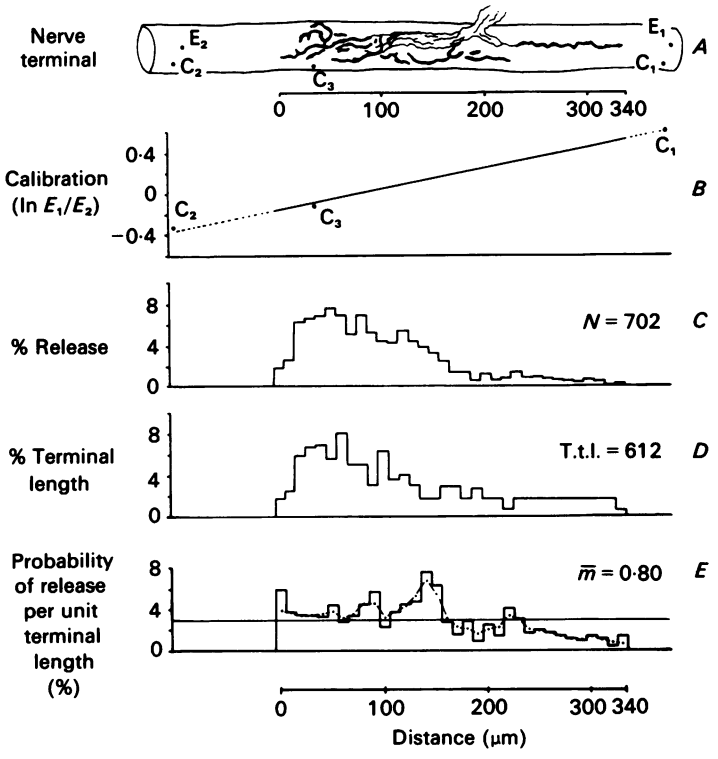

Fig. 6. Characteristic 'complex' terminal which displayed an intricate network of branches heavily biased to the left side of the end-plate. Again there was a good correlation between *C* and *D*. Although release was high around the point of nerve entry it was relatively reduced along the right side of the end-plate. This junction is typical of many in suggesting that the distal drop-off of release may depend upon branch length, with less distal drop-off in short than in long terminal branches. (For a complete description refer to the legend of Fig. 4.)

the terminal. Again, release per unit length was fairly uniform over most of the terminal's length (in this case, about 300 μm of the junction's total 520 μm). It is characteristic of such relatively simple end-plates that most of the central 50–70 % of the junction (or 60–90 % of the total terminal length) shows a fairly uniform release level of perhaps 1·5–2 times the mean, while the distal 15–20 % at each end releases 0·3–0·5 times the mean. Thus the difference between regions of highest and lowest release, for significant stretches of this terminal, was about 5–6-fold. Fig. 10*A* presents another example of such a simple junction, with a clear drop in release probability at both ends.

It is important to point out an artifact that can be generated using our method of analysis. Fig. 5 indicates an apparent sharp peak in release probability at approximately 320–340 μm. This is mainly artifactual, due to the fact that there was a drastically reduced amount of terminal in that 20 μm gap. Given the relatively high release from adjoining parts of the junction, and the $\pm$ 10–20 μm uncertainty in the site of transmitter release inherent in the method, a significant number of events

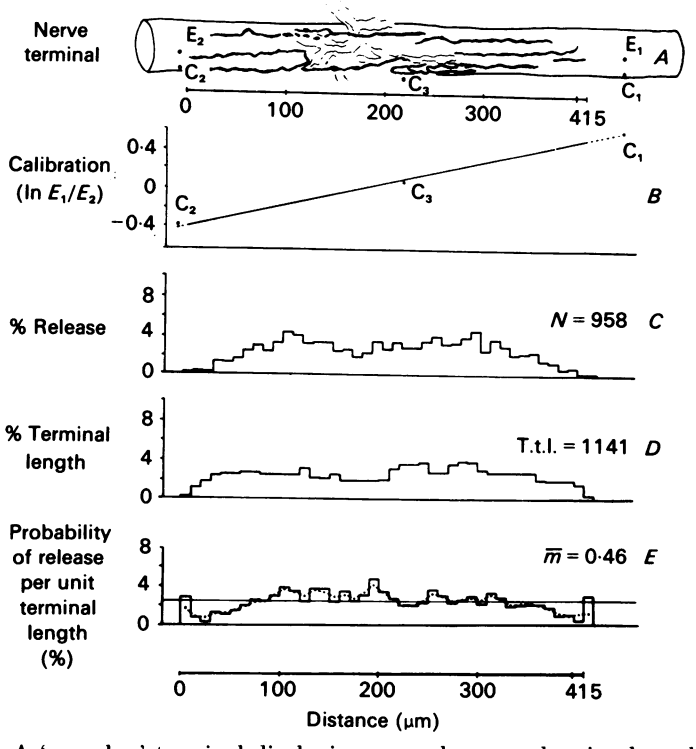

Fig. 7. A 'complex' terminal displaying many long overlapping branches. Release (*C*) closely mimicked terminal length (*D*). Release probability from the central region of the end-plate was highly uniform, but again fell off distally (*E*). The elevated release seen in the end bins was artifactual due to the disproportionally small amount of terminal in those bins (see text for explanation). (See legend of Fig. 4 for complete description.)

would be expected to be mistakenly localized to that 20 μm gap. When the number of these events is divided by the small amount of terminal present in that region, the calculated value for release probability per unit length appears artifactually high. (If there were no terminal within that 20 μm, then release probability would be infinite.) Moreover, it is possible that there may have been more terminal in the gap than we saw. This portion of the junction lay immediately under the myelinated nerve trunk. Nerve terminal and cholinesterase staining are often poor under these conditions, and when the nerve trunk is removed to improve visibility parts of terminal branches can be pulled off as well. For these reasons, it cannot be concluded that the small amount of terminal located at 320–340 μm was releasing at a higher than average level. The same kind of artifact can occur at the ends of junctions (see for example Figs. 6 and 7) where the terminal often occupied only a small portion of a 10 μm bin.

Complex junctions. Figs. 6, 7 and 10*B* illustrate 'complex' terminals, representative of ten examined, in which there was much terminal branching and overlap, but apparently only a single axonal input. Fig. 6 is interesting in showing a highly asymmetric, non-uniform morphological distribution of terminal, while the junction

of Fig. 7 was uniform in terminal distribution but had an unusual number of terminal branches. Again the profiles of percentage terminal length and percentage release per 10 μm bin (Fig. 7 panels *D* and *C* respectively) appear to mimic each other closely, indicating generally uniform release. The probability of release per unit length (panel *E* in both Figs. 6 and 7) showed characteristics like those of simple terminals. In both cases shown there was relatively uniform release from most of the central region of the junction, and a tendency for fall-off of release in the distal 20–30 %. The junction shown in Fig. 6 was exceptional in showing little decrease in release per unit length toward the ends of the short branches on the left side. This may reflect a tendency for short branches to maintain uniform release properties more successfully than long terminals. The junction shown in Fig. 7 had particularly uniform release across its central 300 μm. Unfortunately, we cannot discriminate differences in release among the parallel overlapping branches using this technique; hence it is possible that the apparent uniformity could result from some branches having high levels of release, the parallel ones having low levels of release. On the other hand, it is sometimes possible to make a reasonable guess as to the function of different branches. In the terminal shown in Fig. 10*B* for example, the most obvious interpretation of the release probability pattern for the three branches on the right side of the junction is that the middle branch was still releasing at a normal level beyond the point where the branches to either side showed reduced release and then terminated. Each branch apparently showed a similar drop in release over its distal 20–30 μm of length.

Polyneuronally innervated junctions. In contrast to the properties described above, several fibres ($n = 6$) were encountered that demonstrated conspicuously asymmetrical distribution of release probability. Figs. 8, 9 and 10*C* show three such examples. In these junctions large segments of the terminal released disproportionately small amounts of transmitter. In the junction of Fig. 8 approximately half of the terminal appeared to release about one-third as much transmitter as the other half. Again the distal portion of both sides showed a marked reduction in release probability. In Fig. 9, the portion of the terminal to the right of the 200 μm position released extremely little transmitter, perhaps 5–10 % as much as the left side of the terminal. The junctions shown in Figs. 8, 9 and 10*C* were also characteristic of this category in showing apparent polyneuronal innervation morphologically. All appeared to have more than one myelinated axon branch ending at the junction (possibly three in the case of Fig. 9) and there were discrete portions of the terminal that, if formed by a weaker second axon, could explain the reduced probability of release. After initially encountering this kind of behaviour, attempts were made routinely to determine physiologically the number of inputs to each junction studied. After taking the single quantum release data, we replaced our low calcium Ringer solution with normal Ringer solution (1·8 mM-calcium) and a blocking concentration of curare, and looked for multiple e.p.p. components with different stimulus intensity thresholds. Although some fibres showed such graduated steps of e.p.p. recruitment, and it is known that 30–40 % of the junctions in this size of c.p. are polyneuronally innervated (Trussell & Grinnell, 1985), we could not physiologically differentiate multiple inputs in the fibres illustrated. Although this was the only practical method available for revealing polyneuronal innervation, it is not an adequate one (see Discussion).

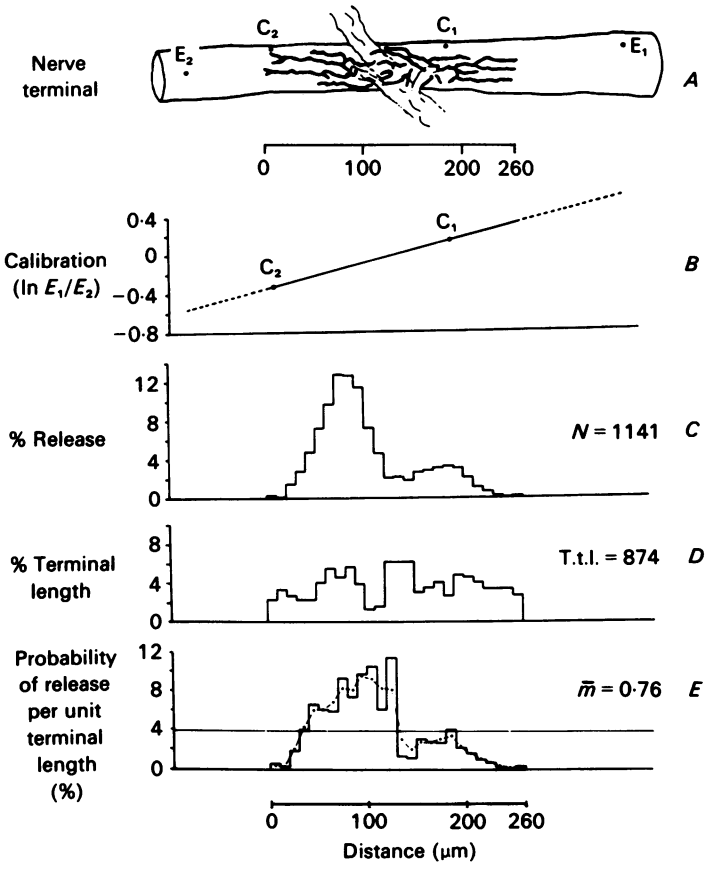

Fig. 8. Characteristic 'polyneuronally innervated' terminal, which displayed a high degree of asymmetry in probability of release per unit length. The left half of this terminal released approximately 3 times more transmitter than the right half (*E*). Although we have no physiological proof for multiple inputs to this end-plate, morphologically there appeared to be two inputs. (For a complete description refer to legend of Fig. 4.)

Clustering of failures and events

It has been claimed that, at any given position along a terminal branch, there is a tendency for stimulus-induced release to occur in temporal clusters, interrupted by series of failures (Vautrin & Mambrini, 1980). If such non-random release occurs routinely, one would not expect the over-all proportion of failures, single and multiple quantum e.p.p.s to satisfy Poisson statistics, which has been shown to be the case in frog neuromuscular junctions at low quantal content (del Castillo & Katz, 1954; Martin, 1977). However, one could imagine subtle oscillations in terminal metabolism that might result in increases and decreases in probability of release, without noticeably affecting the e.p.p. amplitude distribution or absolute numbers of failures. We could easily test for the existence of non-random clustering of release and failures for the junction as a whole at low release levels in our preparations by doing a 'runs

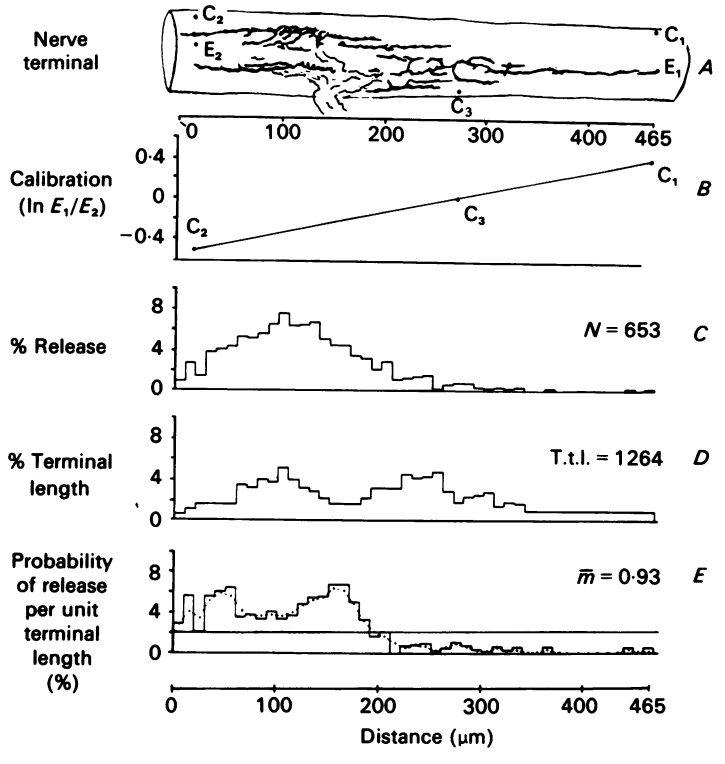

Fig. 9. A possible 'polyneuronally innervated' terminal showing a high degree of asymmetry in release. There appeared to be three myelinated axonal branches ending at this junction. In this case, the region 180–465 μm was relatively 'silent' even though it accounted for 47% of the total terminal length. Clearly different areas within a given end-plate can have dramatically different levels of release. (For a complete description see legend of Fig. 4.)

analysis'. (A run is a series of failures or a series of events, with the shortest run being one event or one failure.) The following equation was used to test our data:

$$Z = -\frac{R-2NP(1-P)}{2\sqrt{N}P(1-P)},$$

where N is the total number of records, P is the probability of an event, whether it be unit or multi quantal, and R is the number of runs. Alternating failures and events would yield the largest value of R. In our experiments, P was determined as the number of events per N. A standardized random variable (Z) can then be calculated. Our data were found to have Z values of less than 1 ($-1{\cdot}1$, $+0{\cdot}51$, $+0{\cdot}74$, $-0{\cdot}55$ and $-0{\cdot}10$), which, judged by a one-tailed test, indicates no statistically non-random clustering ($P > 0{\cdot}10$). An excellent presentation of this method is given by Horn, Vandenberg & Lange (1984).

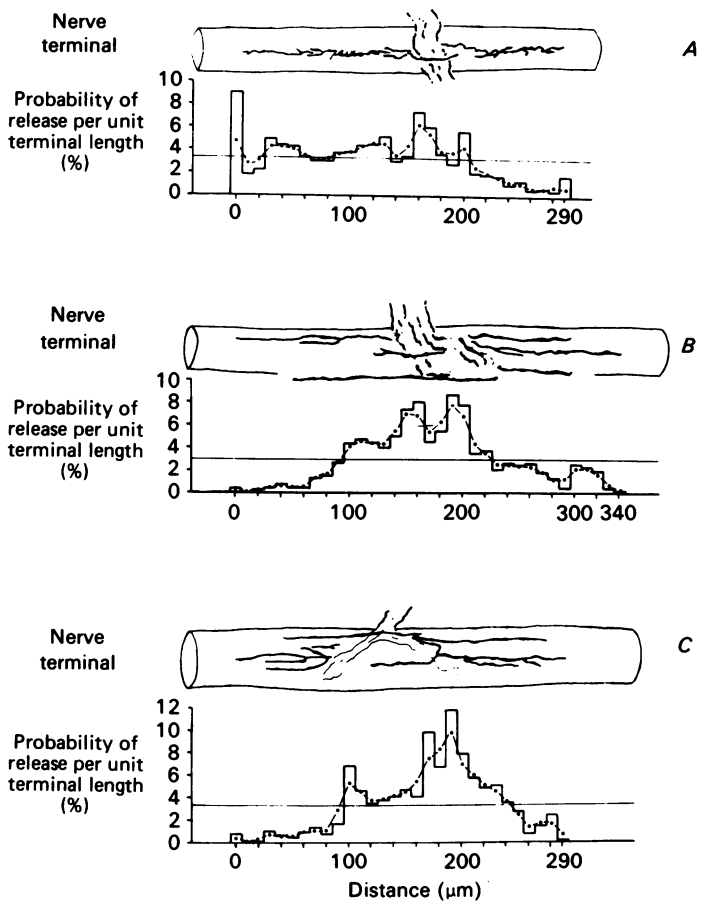

Fig. 10. A composite of three end-plates characterized as 'simple' (*A*), 'complex' (*B*) and 'possibly polyneuronally innervated' (*C*). This Figure reinforces the general finding that release is highest near the point of nerve entry and is reduced towards distal ends. *A*: total terminal length (t.t.l.) = 421 μm, number of records (N) = 713, mean quantal content ($\overline{m}$) = 2·9. *B*: t.t.l. = 795 μm, N = 1131, $\overline{m}$ = 0·59. *C*: t.t.l. = 763 μm, N = 427, $\overline{m}$ = 0·50. Data are presented as in panels *A* and *E* of Fig. 4 for each terminal.

Independence of release from different sites

Another question is whether release from one site influences release from the same or neighbouring sites on subsequent stimulation, for example under conditions of facilitation. We have looked for evidence of such interaction among pairs of single quantum e.p.p.s evoked at 40 ms intervals, one pair per second. A separation of 40 ms was sufficient to ensure separation of unit quantal responses, while still producing 20–50 % facilitation in the second response. Table 1 summarizes the frequency at which a single quantum response to the second stimulus came from within ± 20 μm of the same location as a single quantum response to a stimulus 40 ms earlier. (A value of ± 20 μm was chosen in order to obtain the highest degree of confidence in saying whether the second site of release could have been the 'same' or had to be different

than the first.) Six experiments were assayed, in which the quantal content to the second stimulus in the pair showed a mean 34% facilitation. We also looked for interaction between consecutive unit quantal events at a stimulus interval of 1 s, when no facilitation remains, and, as a control, we looked for evidence of release from the same site ($\pm 20\ \mu$m) when single quantum events from the first half of the

TABLE 1. Test of the effect of single quantum release on location of release of a subsequent single quantum of transmitter

Experiment	*% facilitation at 40 ms interval	% of second events arising within $\pm 20\ \mu$m of the first†		
		at 40 ms	at 1 s	40 ms/1 s
1	22	20·2	23·4	0·86
2	35	17·5	20·7	0·85
3	53	34·8	31·2	1·12
4	36	18·3	21·9	0·84
5	40	13·8	16·4	0·84
6	18	14·6	14·6	1·0
Mean	34%	19·9	21·4	0·92

* Based on mean quantal content for first and second responses in all pairs given ($n > 3000$).

† Random comparison of the sites of release of unit quantal events in the first and second halves of each experiment yielded a mean probability of 19·6% that any two events arose within $\pm 20\ \mu$m of each other.

experiment were compared randomly with single quantum events occurring during the second half of the experiment, at a mean separation of 20 min or more. We conclude from Table 1 that there is no evidence that release of a quantum has any influence on the site of release of another quantum 40 ms or 1 s later.

This conclusion is reinforced by comparison of the release profiles of terminals to the first and second stimuli of the 40 ms pair. Although the second stimuli showed a higher probability of release, the profile of probability of release from different parts of the terminal is essentially the same as that to the first stimulus of the pair. At least at a 40 ms interval, with only mild facilitation, there is no perceptible tendency for disproportionately increased release from the distal portions of terminals.

Quantal size as a function of site of release

Our data also allow us to determine the absolute size of each single quantum e.p.p., by correcting the measured amplitude for the length constant of the fibre and the distance from either recording electrode (in our case E_2). Since there have been reports that different portions of a terminal can release quanta of different mean size, as judged by m.e.p.p. amplitude (Bennett & Pettigrew, 1975; Bieser, Wernig & Zucker, 1984), we have examined this parameter as well, to determine the variability in amplitude of single quantum e.p.p.s known to have been released from a restricted portion of a single branch. In the several cases we have examined, the variability in unit quantal e.p.p. size from restricted portions of a single branch was essentially as great as that from the entire terminal. Fig. 11 shows the amplitude distributions of

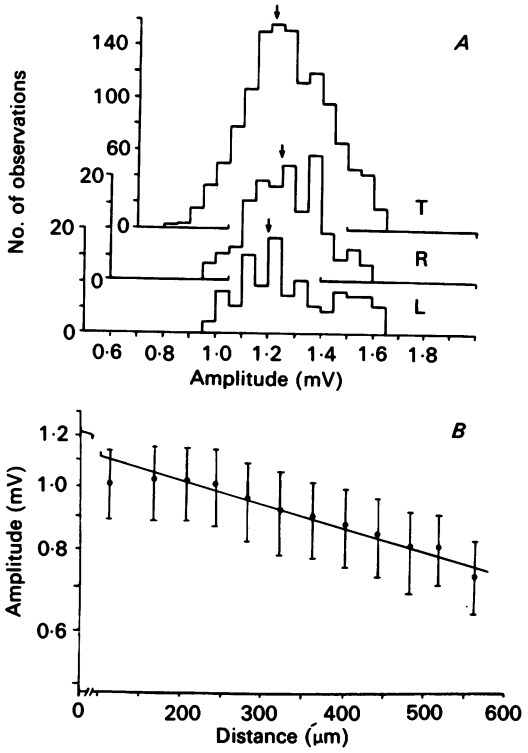

Fig. 11. Distribution of absolute unit quantal sizes referred to distance from recording electrode E_2 for a 'simple' terminal (see Fig. 8). *A* shows histograms of events corrected to their absolute amplitude at the site of origin from the whole terminal (T), from a 40 μm segment on the right side (R) of the terminal (160–200 μm) and from a comparable segment on the left side (L) (360–400 μm). Restricted segments were sampled because a sufficient number of responses could be obtained from a relatively simple portion of one branch. Distribution of R and L are similar to T and mean values (arrows) are almost identical: $1{\cdot}22 \pm 0{\cdot}16$, $1{\cdot}25 \pm 0{\cdot}13$ and $1{\cdot}20 \pm 0{\cdot}17$ for T, R and L, respectively. *B*, a plot of recorded (not corrected) unit quantal amplitudes as a function of distance from E_2. Note the large standard deviations, reflecting the wide range in amplitude shown in *A*. This variability is essentially equivalent at all points, but over most of the junctional length the means changed with distance in a way consistent with cable properties of the fibre (continuous line). At the ends of this terminal, as well as of several others studied, the mean amplitude appeared lower than predicted by this relationship, suggesting that quantal events may be reduced in size at the ends of junctions.

single quantum e.p.p.s recorded from a whole junction and from two restricted 40 μm segments of the fibre at opposite ends of the junction. All amplitudes were corrected for decrement due to their distance from the recording electrode. This Figure is taken from the junction shown in Fig. 5, and the two restricted portions were from 160–200 μm and 360–400 μm, i.e. from short segments of single terminal branches. It is clear that both distributions are virtually the same, and both have essentially the same mean and approximate distribution of amplitudes as are seen in the total terminal. When e.p.p. amplitude distributions were plotted for successive 40 μm segments of the junction, without correction for decrement due to distance, the mean

amplitude of each point shifted almost exactly as predicted on the basis of distance from the electrode and the length constant of the fibre (Fig. 11 *B*). The only exceptions to this were at the distal ends of some junctions, where there was a decrease in mean single quantum amplitude. There were fewer e.p.p.s to average at the ends, but the drop in mean amplitude distally was observed in seven of fifteen ends of junctions examined in this respect. There was never an increase in mean amplitude distally, although several junctions showed no deviation from the values predicted from cable theory.

In junctions with suspected polyneuronal innervation, it was of interest to determine the mean single quantum amplitudes from the parts of the junction apparently formed by different myelinated axon branches. Again, despite possible different origin of different parts of the terminal, and grossly different release levels, the mean absolute amplitudes and the amplitude distributions were essentially indistinguishable for the different components of the junction. In the junction shown in Fig. 8, for example, the mean absolute amplitude $\pm$ S.D. for the portions at distance 0–120 μm was $1{\cdot}59 \pm 0{\cdot}24$ mV ($n = 899$), and at 120–260 μm was $1{\cdot}60 \pm 0{\cdot}22$ mV ($n = 242$) respectively. In the junction shown in Fig. 9, the part of the junction at 0–210 μm had a single quantum mean of $1{\cdot}12 \pm 0{\cdot}16$ mV ($n = 617$) while the nearly 'silent' portion at 220–465 μm had a quantal size $1{\cdot}14 \pm 0{\cdot}13$ mV ($n = 36$). In short, while there is a wide (and unexplained) range of single quantum e.p.p. amplitudes, we see no evidence that within a given junction the size differs as a function of branch of origin, or point along a branch, except perhaps in the distant 20–30 μm of some, but not all, branches.

DISCUSSION

We have shown that by using an intracellular recording method it is possible to determine the site of origin of a single quantum e.p.p. along the length of the fibre with an accuracy of approximately $\pm$10–20 μm. Since our results differ in significant ways from those obtained with extracellular recording of end-plate currents (Bennett & Lavidis, 1979, 1982; Bieser *et al.* 1984), it is appropriate to consider the advantages and disadvantages of each method, and the reasons for adopting the technique we have used.

Extracellular recordings, especially with pairs of electrodes located close to one another and closely apposed to a terminal branch, are able to localize release with considerably greater accuracy than our intracellular technique, probably to within ± 5 μm (del Castillo & Katz, 1956; Bieser *et al.* 1984). However, such close apposition of recording electrodes to the terminal can affect release, usually inducing abnormally high levels due to direct distortion of the terminal by the electrode or via tension on the connective tissue (del Castillo & Katz, 1956; Katz & Miledi, 1973; Wernig, 1976). It is necessary to control for such distortion by intracellular measurement of quantal content and m.e.p.p. frequency throughout an experiment. However, even with this control, there might be a danger that subtle alterations of membrane properties might affect evoked release from a very localized spot without grossly changing quantal content, or that action potential invasion distal to the electrode could be affected. If this problem is minimized by using a large extracellular electrode, located safely off the terminal itself, the accuracy of localization is much less, with

events recordable up to 20–40 μm distant from the site of release, depending on the exact electrode position and terminal gutter geometry (del Castillo & Katz, 1956; Katz & Miledi, 1965; Wernig, 1976; Bieser *et al.* 1984). Moreover, terminals are much easier to visualize and extracellular recordings much easier to achieve when the surface has been cleaned enzymatically, which can affect contact between the terminal and the muscle fibre. It is usually feasible only to sample one extracellular site at a time; hence if several spots are to be monitored they must be studied sequentially. Since only a small fraction of the whole junction can normally be seen in the living preparation, it is impossible to sample from all representative portions of the terminal. Moreover, it is difficult to be confident of a recording position if no activity is seen. Finally, to study evoked release with an extracellular electrode the quantal content must be high enough for a significant number of events to occur near the electrode. With quantal contents of two or higher, however, it is difficult to resolve single events with an intracellular electrode in order to know the true amplitude of the event recorded extracellularly. At higher quantal contents it is also difficult to be confident that an extracellularly recorded event is single rather than the result of multiple release of quanta within recording distance of the electrode.

The intracellular recording technique we have used offers several advantages. It allows localization of virtually *all* single quantum events along the entire length of the terminal during a given time period. It requires no close probing within the confines of the junction itself, at least until the calibration is done, near the end of an experiment. It allows knowledge of the true amplitude of each single quantum event, and study of evoked release at low enough release levels so that synaptic depression is avoided (Rahamimoff, 1968). Finally, the amplitude ratio method we have used approximates the accuracy of localization using extracellular techniques. On the other hand, our technique has limitations: it requires stable penetrations by two electrodes for an hour or more; it does not allow one to distinguish between release from different terminal branches that run parallel to one another, equidistant from the two electrodes; and it is useful only for single quantum e.p.p.s, requiring that one works at low quantal content levels. Nevertheless, within these limits it provides an accurate and complete profile of release probability.

In contrast to the results of Bennett & Lavidis (1979), our data are not supportive of the idea that there are single active zones, or even localized regions of approximately 20–30 μm of terminal, that release grossly larger amounts of transmitter than do most other parts of the terminal. It is quite possible, however, that an extracellular recording electrode located in an area of high terminal density (multiple branches), and recording events from $\pm$15–30 μm, could 'see' as much as 50% of the total terminal release. This might be one explanation for the result of Bennett & Lavidis (1979).

In general, our data suggest that release from the central 50–70% of the end-plate length, which represents about 60–90% of the summed terminal branch length, is relatively uniform, but that release decreases distally, especially in the longest branches of the terminal. In some cases, the distal ends can be virtually 'silent' under our conditions, releasing only 5–10% as much transmitter as the central region. Thus our findings support the conclusion of Bennett & Lavidis (1982) that release frequently decreases distally in a terminal branch. On the other hand, we do not

always see such a decrease, especially occurring as close to the point of nerve entry as was observed by Bennett & Lavidis (1982). In the terminals we have studied, release is often approximately uniformly high for as much as 150–200 μm from the point of nerve entry. We have no explanation for this difference in findings, unless the low absolute concentration of divalent cations (0·35 mM) in their preparation might have contributed, for example, by affecting action potential invasion.

The decrease in probability of release distally in terminal branches is of obvious interest. Several possible explanations can be envisioned. Likely candidates include: (1) a decrease distally in number or size of active zones, or a paucity of some other critical release component, such as calcium channels; (2) a lengthwise gradient in terminal calcium pumping or buffering, in membrane potential or in coupling of calcium conductance to potential change, and/or (3) a change in the properties of the action potential as it propagates distally.

Davey & Bennett (1982) have reported a consistent decrease in terminal diameter with distance along the terminal that could help explain the distal drop in release. However, a more thorough study of the ultrastructure of physiologically identified sartorius junctions yielded no evidence for systematic changes in the diameter or synaptic contact area of terminal branches along their length (A. A. Herrera, A. D. Grinnell & B. Wolowske, unpublished; Werle, Herrera & Grinnell, 1984). On the other hand, it is quite possible that physiological differences may be involved (cf. Grinnell & Herrera, 1980, 1981). There is evidence that terminals with high levels of transmitter release per unit length differ from those with low release per unit length in having a higher concentration of active calcium ions inside the resting terminal, and a higher influx of calcium ions in response to action potential invasion (possibly reflecting differences in density of calcium channels (Pawson & Grinnell, 1984)). If such differences can exist along the length of terminals, it could help explain the gradient of release we observe. In addition, a proximal–distal gradient in excitability of frog motor nerve terminals could explain the drop-off in release distally. Most evidence suggests that there is action potential invasion to the end of frog terminals (Katz & Miledi, 1965, 1968; Braun & Schmidt, 1966; Gunderson *et al.* 1981), and that a block of conduction, by tetrodotoxin (TTX) application, causes rapid disappearance of release distal to the block (Katz & Miledi, 1968). Since evoked release can be seen in distal portions of branches, it is unlikely that there is complete failure of invasion, analogous to that seen with TTX block. However, Mallart (1984) has presented evidence for a reduced density of sodium channels in the distal portion of branches. This would be expected to lead to reduced action potential amplitude and reduced release, and might also help to explain the release profiles seen by us and Bennett & Lavidis (1982).

Finally, it is worth noting also that release from developing and regenerating terminals is often reduced, correlated with poorly organized active zone structure (Ko, 1981) and probably with other differences in mature terminals. Since it is now clear that frog terminals regularly undergo remodelling changes in the form of terminal retraction and regrowth (Wernig *et al.* 1980; Anzil, Bieser & Wernig, 1984), it is possible that distal portions of many terminals may represent regressing or immature, newly formed structures.

Perhaps the most interesting finding of this study is the existence of junctions with

highly asymmetric profiles of probability of release per unit length. In these cases, a large percentage of the terminal was found to release much less than the rest of the terminal. Since these were usually junctions that appeared, morphologically, to be innervated by more than one myelinated axon branch, we suspect that they were polyneuronally innervated junctions in which one of the inputs was very much weaker than the other. In most such cases, including those of Figs. 8, 9 and 10*C*, we were unable to demonstrate independent axonal inputs by varying stimulus intensity in normal Ringer solution plus curare. However, this is not compelling evidence that only one axon was involved, for several reasons: (1) if weaker inputs came from neurones with higher thresholds, they could be lost in the larger event; (2) axons may have similar thresholds, making stimulus intensity discrimination difficult or impossible; (3) weak junctions may be totally blocked by the curare concentration used. If more than one axon was involved, it demonstrates that large terminals constituting as much as 50 % of the input to a junction can be relatively 'silent'. This has interesting implications for the process of synapse elimination. Clearly, weak inputs need not be correspondingly small, morphologically, nor do they necessarily look thinner or otherwise different than strong inputs. Alternatively, if in fact only one neurone is involved, then our data would indicate that different branches of the same axon, at the same junction, can release dramatically different amounts of transmitter per unit length. In light of the fact that different terminals of the same axon on different fibres may vary greatly in release per unit length (Trussell & Grinnell, 1985; B. M. Nudell, unpublished observations), it is possible that one axon could form such diverse terminal components at the same junction. We consider it more likely that two neurones are involved, but the question must be resolved by further experimentation. Whichever is the case, it is clear that determinations of a mean value for release per unit length from a whole junction must be interpreted cautiously.

We see no evidence for fluctuations in release probability with time for the terminal as a whole, i.e. the incidence of clusters of successive failures or events was consistent with predictions made on the basis of random occurrence of e.p.p.s and failures at mean frequencies appropriate to the junctions' quantal contents.

It is also possible, in our preparations, to ask whether there is any 'cooperativity' in release. Vautrin & Mambrini (1980) have reported that single quantum e.p.p.s at frog junctions occur in discrete latency steps, and that successive responses at 1–10 Hz often show non-random clustering at first one latency, then another. This could imply that release occurs selectively at only a few discrete spots, and that release at one site increases the probability of subsequent release from the same site. Again, our data do not support this conclusion. When we examined the probability of release being from the same approximate part of the junction (± 20 μm) as an event 40 ms or 1 s earlier, and compared this with the probability of two randomly compared single quantum events coming from the same area, the probabilities were all about the same (Table 1). Thus we conclude that, in the terminals we have examined, release occurs independently of the preceding event. This is in agreement with the results of Barrett & Stevens (1972), who demonstrated mutual independence between release sites.

Finally, it is of interest to consider the size of single quantum events. In their

pioneering study of m.e.p.p. amplitudes, del Castillo & Katz (1954, 1956) (see also Fatt & Katz, 1951) noted that variability in these values was much greater than would be expected from cable properties alone. Our results verify that this variability is not the result of differential decrement in amplitude of similar-sized single quantum e.p.p.s arising at different distances from the recording electrodes. Even the events arising from a restricted part of one branch of a terminal varied over the same wide amplitude range. The explanations for this variability in unit event size at any given point along a terminal are unknown, and could be presynaptic or post-synaptic. This has been a subject of interest since the initial findings of del Castillo & Katz (1954). Our data do not provide information concerning this issue.

On the other hand, our findings do address the question of uniformity of quantal size at different parts of a junction. There have been reports that different branches of a terminal, or different portions of a branch, can give rise to m.e.p.p.s of different characteristic amplitude. Bennett & Pettigrew (1975) reported that this was the case in developing sartorius nerve terminals, and that differences in quantal size could be correlated with differences in vesicle size. More recently, Bieser *et al.* (1984) have reported that different branches of the same terminal, especially those that might represent newly formed or remodelled components (ends of branches or isolated varicosities), sometimes evoked single quantum e.p.p.s of different mean amplitude. Our results are consistent with the possibility of a slight drop in mean amplitude at distal ends of branches, although the variability at all points is so great that any such mean difference is small by comparison. One possible artifactual explanation for such an observation would be that close to a recording electrode in a large fibre, the decay in amplitude with distance is steeper than predicted for a simple linear cable (Fatt & Katz, 1953). However, that effect was important only in larger fibres than we have used, and at points very close to the recording electrode, so we consider it unlikely that it is the source of the distal decline in amplitude we observed. For most of the length of the terminals studied the mean amplitude was remarkably constant, even in junctions where part of the terminal was releasing at a much higher level than another part. Apparently post-synaptic sensitivity does not differ as a function of activity levels in such cases.

We thank Dr Michael Delay for essential help in computer programming, Frances Knight, Brad Smith and Don Curtis for technical assistance, Sandra Nath Singh for helping to prepare the manuscript, and Drs Albert Herrera, Frank Krasne, Michael Letinsky and Bruce Nudell for constructive criticisms and comments. This work was supported by NIH and MDA Fellowships to A.J.D. and by research grants from NIH (NS06232) and the MDA.

REFERENCES

ANZIL, A. P., BIESER, A. & WERNIG, A. (1984). Light and electron microscopic identification of nerve terminal sprouting and retraction in normal adult frog muscle. *Journal of Physiology* **350**, 393–399.

BARRETT, E. F. & STEVENS, C. F. (1972). Quantal independence and uniformity of presynaptic release kinetics at the frog neuromuscular junction. *Journal of Physiology* **277**, 665–689.

BENNETT, M. R. & LAVIDIS, N. A. (1979). The effect of calcium ions on the secretion of quanta evoked by an impulse at nerve terminal release sites. *Journal of General Physiology* **74**, 429–456.

BENNETT, M. R. & LAVIDIS, N. A. (1982). Variation in quantal secretion at different release sites along developing and mature motor terminal branches. *Developmental Brain Research* **5**, 1–9.

BENNETT, M. R. & PETTIGREW, A. G. (1975). The formation of synapses in amphibian striated muscle during development. *Journal of Physiology* **252**, 203–239.

BIESER, A., WERNIG, A. & ZUCKER, H. (1984). Different quantal responses within single frog neuromuscular junctions. *Journal of Physiology* **350**, 401–412.

BRAUN, M. & SCHMIDT, R. F. (1966). Potential changes recorded from the frog motor nerve terminal during its activation. *Pflügers Archiv für die gesamte Physiologie des Menschen und der Tiere* **287**, 56–80.

COUTEAUX, R. & PÉCOT-DECHAVASSINE, M. (1970). Vésicules synaptiques et poches au niveau de les 'zones actives' de la junction neuromusculaire. *Comptes rendus hebdomadaire des séances de l'Académie des sciences* **271**, 2346–2349.

D'ALONZO, A. J. & GRINNELL, A. D. (1982). Uniformity of transmitter release along the length of frog motor nerve terminals. *Neuroscience Abstracts* **8**, 493.

DAVEY, D. F. & BENNETT, M. R. (1982). Variation in the size of synaptic contacts along developing and mature motor terminal branches. *Developmental Brain Research* **5**, 11–22.

DEL CASTILLO, J. & KATZ, B. (1954). Quantal components of the end-plate potential. *Journal of Physiology* **124**, 560-573.

DEL CASTILLO, J. & KATZ, B. (1956). Localization of active spots within the neuromuscular junction of the frog. *Journal of Physiology* **132**, 630–649.

FATT, P. & KATZ, B. (1951). An analysis of the end-plate potential recorded with an intracellular electrode. *Journal of Physiology* **115**, 320–370.

FATT, P. & KATZ, B. (1953). The electrical properties of crustacean muscle fibres. *Journal of Physiology* **120**, 171–204.

GRINNELL, A. D. & HERRERA, A. A. (1980). Physiological regulation of synaptic effectiveness at frog neuromuscular junctions. *Journal of Physiology* **307**, 301–317.

GRINNELL, A. D. & HERRERA, A. A. (1981). Specificity and plasticity of neuromuscular connections: long-term regulation of motoneuron function. *Progress of Neurobiology* **17**, 203–282.

GUNDERSON, C. B., KATZ, B. & MILEDI, R. (1981). The reduction of end-plate responses by botulinum toxin. *Proceedings of the Royal Society* B **213**, 489–493.

HARRIS, J. B. & RIBCHESTER, R. R. (1979). The relationship between end-plate size and transmitter release in normal and dystrophic muscles of the mouse. *Journal of Physiology* **296**, 245–265.

HERRERA, A. A. & GRINNELL, A. D. (1980). Transmitter release from frog motor nerve terminals depends on motor unit size. *Nature* **287**, 649–651.

HERRERA, A. A. & GRINNELL, A. D. (1981). Contralateral denervation causes enhanced transmitter release from frog motor nerve terminals. *Nature* **291**, 495–497.

HERRERA, A. A., GRINNELL, A. D. & WOLOWSKE, B. (1983). Ultrastructural correlates of differences in synaptic effectiveness at frog neuromuscular junctions. *Neuroscience Abstracts* **9**, 1026.

HEUSER, J. E. & REESE, T. S. (1973). Evidence for recycling of synaptic vesicle membrane during transmitter release at the frog neuromuscular junction. *Journal of Cell Biology* **57**, 315–344.

HEUSER, J. E., REESE, T. S., DENNIS, M. J., JAN, Y., JAN, L. & EVANS, L. (1979). Synaptic vesicle exocytosis captured by quick freezing and correlated with quantal transmitter release. *Journal of Cell Biology* **81**, 275–300.

HODGKIN, A. L. & RUSHTON, W. A. H. (1946). The electrical constants of a crustacean nerve fibre. *Proceedings of the Royal Society* B **133**, 444–479.

HORN, R., VANDENBERG, C. A. & LANGE, K. (1984). Statistical analysis of single sodium channels: effects of *N*-bromoacetamide. *Biophysical Journal* **45**, 323–335.

JACK, J. J. B., NOBLE, D. & TSIEN, R. W. (1975). Linear cable theory. In *Electric Current Flow in Excitable Cells*, pp. 25–66. Oxford: Oxford University Press.

KATZ, B. (1948). The electrical properties of the muscle fibre membrane. *Proceedings of the Royal Society* B **135**, 506–534.

KATZ, B. & MILEDI, R. (1965). Propagation of electric activity in motor nerve terminals. *Proceedings of the Royal Society* B **161**, 453–482.

KATZ, B. & MILEDI, R. (1968). The effect of local blockage of motor nerve terminals. *Journal of Physiology* **199**, 729–741.

KATZ, B. & MILEDI, R. (1973). The binding of acetylcholine to receptors and its removal from the synaptic cleft. *Journal of Physiology* **231**, 549–574.

KARNOVSKY, M. J. (1964). The localization of cholinesterase activity in rat cardiac muscle by electron microscopy. *Journal of Cell Biology* **23**, 217–232.

KO, C.-P. (1981). Electrophysiological and freeze-fracture studies of changes following denervation at frog neuromuscular junctions. *Journal of Physiology* **321**, 627–639.

KUNO, M., TURKANIS, S. A. & WEAKLY, J. N. (1971). Correlation between nerve terminal size and transmitter release at the neuromuscular junction of the frog. *Journal of Physiology* **213**, 545–556.

LETINSKY, M. S. & DECINO, P. (1980). Histological staining of pre- and postsynaptic components of amphibian neuromuscular junctions. *Journal of Neurocytology* **9**, 303–320.

MALLART, A. (1984). Presynaptic currents in frog motor endings. *Pflügers Archiv* **400**, 8–13.

MARTIN, A. R. (1977). Junctional transmission: presynaptic mechanisms. In *Cellular Biology of Neurons*, part 1, *The Nervous System*, ed. KANDEL, E. R., pp. 329–355. American Physiological Society.

NUDELL, B. M. & GRINNELL, A. D. (1982). Inverse relationship between transmitter release and terminal length in synapses on frog muscle fibers of uniform input resistance. *Journal of Neuroscience* **2**, 216–224.

NUDELL, B. M. & GRINNELL, A. D. (1983). Regulation of synaptic position, size, and strength in anuran skeletal muscle. *Journal of Neuroscience* **3**, 161–176.

PAWSON, P. A. & GRINNELL, A. D. (1984). Post tetanic potentiation in strong and weak neuromuscular junctions: physiological differences caused by a differential Ca^{2+} influx. *Brain Research* (in the Press).

PEPER, K., DREYER, F., SANDRI, C., AKERT, K. & MOOR, H. (1974). Structure and ultrastructure of frog motor endplate. *Cell and Tissue Research* **149**, 437–455.

POCKETT, S. & SLACK, J. R. (1982). Pruning of axonal trees results in increased efficacy of surviving nerve terminals. *Brain Research* **243**, 350–353.

RAHAMIMOFF, R. (1968). A dual effect of calcium ions on neuromuscular facilitation. *Journal of Physiology* **195**, 471–480.

TRUSSELL, L. O. & GRINNELL, A. D. (1985). The regulation of synaptic strength within motor units of the frog cutaneous pectoris muscle. *Journal of Neuroscience* (in the Press).

VAUTRIN, J. & MAMBRINI, J. (1980). Spatiotemporal characteristics of the evocated neurotransmitter secretion at the frog neuromuscular junction. In *Ontogenesis and Functional Mechanisms of Peripheral Synapses*, INSERM Symposium no. 13, ed. TAXI, J., pp. 191–198. Amsterdam: Elsevier/North-Holland Biomedical Press.

WERLE, M. J., HERRERA, A. A. & GRINNELL, A. D. (1984). Ultrastructural uniformity along branches of frog motor nerve terminals. *Neuroscience Abstracts* **10**, 919.

WERNIG, A. (1976). Localization of active sites in the neuromuscular junction of the frog. *Brain Research* **118**, 63–72.

WERNIG, A., PÉCOT-DECHAVASSINE, M. & STORER, H. (1980). Sprouting and regression of the nerve at the frog neuromuscular junction in normal conditions and after prolonged paralysis with curare. *Journal of Neurocytology* **9**, 277–303.